HHS Public Access

Author manuscript

Ophthalmol Retina. Author manuscript; available in PMC 2020 December 01.

Published in final edited form as:

Ophthalmol Retina. 2019 December ; 3(12): 1056–1066. doi:10.1016/j.oret.2019.06.010.

Higher Order Assessment of OCT in Diabetic Macular Edema from the VISTA Study: Ellipsoid Zone Dynamics and the Retinal Fluid Index

Justis P. Ehlers[1,2,*], **Atsuro Uchida**[1,2,*], **Ming Hu**[1,3], **Natalia Figueiredo**[1,2], **Peter K. Kaiser**[2], **Jeffrey S. Heier**[4], **David M. Brown**[5], **David S. Boyer**[6], **Diana V. Do**[7], **Andrea Gibson**[8], **Namrata Saroj**[8], **Sunil K Srivastava**[1,2]

[1]The Tony and Leona Campane Center for Excellence in Image-Guided Surgery and Advanced Imaging Research, Cole Eye Institute, Cleveland Clinic, 9500 Euclid Ave, Cleveland, OH 44195

[2]Cole Eye Institute, Cleveland Clinic, 9500 Euclid Ave/i32, Cleveland, OH 44195

[3]Department of Quantitative Health Sciences, Lerner Research Institute, Cleveland Clinic, 9500 Euclid Ave, Cleveland, OH 44195, USA

[4]Ophthalmic Consultants of Boston, Boston, MA

[5]Retina Consultants of Houston, Houston, TX

[6]Retinal-Vitreous Associates, Los Angeles, CA

[7]Byers Eye Institute, Stanford University, Palo Alto, CA

[8]Regeneron Pharmaceuticals, Tarrytown, NY

Abstract

Objective: To investigate retinal fluid features and ellipsoid zone (EZ) integrity dynamics on spectral domain optical coherence tomography (SD-OCT) in eyes with diabetic macular edema (DME) treated with intravitreal aflibercept injection (IAI) in the VISTA-DME study.

Design: A post-hoc subanalysis of phase III, prospective clinical trial.

Correspondence to: Justis P. Ehlers, MD, Cole Eye Institute, Cleveland Clinic, 9500 Euclid Avenue/i32, Cleveland, OH 44195, ehlersj@ccf.org, Tel: +1-216-636-0183.

*Co-First Authors

Competing interests: JPE: Bioptigen (C, P), Synergetics (P), Leica (C), Carl Zeiss Meditec (C).

Disclosures: **JPE**: Bioptigen/Leica (C, P), Thrombogenics (C, R), Genentech (C, R), Roche (C), Aerpio (C, R), Alcon (C, R), Novartis (C,R), Allergan (C), Allegro (C), Boehringer Ingelheim (R), Regeneron (C,R), Zeiss (C); **AU:** None; **MH**: None; **NF**: None; **PKK:** Alcon (C), Bayer (C); Regeneron (C); Novartis (C); Allegro (C); Allergan (C); **JSH:** Aerpio (C); Allergan (R, C); Bayer (C); Novartis (R, C); Regeneron (R, C); Genentech (C, R); Allegro (C); Alcon (R), Sanofi (C, R); **DMB:** Alcon (C, R) Allergan (R, C); Bayer (C); Clearside Biomedical (C); Zeiss (C); Heidelberg (C), Novartis (R, C); Regeneron (R, C); Genentech (C, R); Allegro (R), Santen (R); **DSB:** Bayer (C); Regeneron (R, C); Novartis (C); Allergan (C, R); Genentech (C, R); **DVD:** Santen (C); Regeneron (R); Genentech (R); **AG:** Regeneron (E); **NS**: Regeneron (E); **SKS:** Bioptigen/Leica (P), Allergan (R), Bauch and Lomb (C); Santen (C); Sanofi (C);

Subjects: Eyes received either IAI 2 mg every 4 weeks (2q4) or every 8 weeks after 5 initial monthly doses (2q8).

Methods: All eyes from the VISTA Phase III study in the IAI groups imaged with the Zeiss Cirrus HDOCT system were included. The OCT macular cube datasets were evaluated using a novel software platform to generate retinal layer and fluid boundary lines that were manually corrected for assessment of change in EZ parameters and volumetric fluid parameters from baseline. The retinal fluid index (i.e., proportion of the retinal volume consisting of cystic fluid) was also calculated at each timepoint.

Main Outcome Measures: The feasibility of volumetric assessment of higher order OCT-based retinal parameters and its correlation with best corrected visual acuity (BCVA).

Results: Overall, 106 eyes of 106 patients were included. Specifically, 52 eyes of 52 patients were included in IAI 2q4 arm, and 54 eyes of 54 patients were included in IAI 2q8 arm. EZ integrity metrics significantly improved from baseline to week 100 including central macular mean EZ to retinal pigment epithelium thickness (RPE; 2q4; 26.6 μm to 31.6 μm, $P < .001$, 2q8; 25.2 μm to 31.4 μm, $P < .001$). At week 100, central macular intraretinal fluid volume was reduced by over 65 % ($P < .001$) and central macular subretinal fluid volume was reduced by over 99% in both arms ($P < .001$). Central macular RFI significantly improved in both arms (2q4; 17.9 % to 7.2 %, $P < .001$, 2q8; 19.8 % to 4.2 %, $P < .001$). Central macular mean EZ-RPE thickness (i.e., a surrogate for photoreceptor outer segment length) and central RFI were independently correlated with BCVA at multiple follow-up visits.

Conclusions: IAI resulted in significant improvement in EZ integrity and quantitative fluid metrics in both 2q4 and 2q8 arms and correlated with visual function.

Precis:

Ehlers JP et al, “Higher Order Assessment of Optical Coherence Tomography in Diabetic Macular Edema from the VISTA Study: New Insights in Ellipsoid Zone Dynamics and the Retinal Fluid Index”

In the Phase III VISTA DME trial, ellipsoid zone integrity and retinal fluid index (i.e., proportion of retinal volume consisting of cystic fluid) are both indepdently associated with visual acuity.

Keywords

Optical coherence tomography; diabetic macular edema; ellipsoid zone; retinal fluid

INTRODUCTION

Diabetic retinopathy (DR) is progressive dysfunction of the retinal microvasculature closely associated with chronic hyperglycemia.[1] It is a leading cause of severe visual impairment among working populations worldwide, affecting one-third of an estimated 422 million individuals with diabetes as of 2014.[2, 3] Diabetic macular edema (DME) remains the most frequent cause of moderate vision loss in eyes with DR, characterized by excessive retinal vascular permeability resulting in accumulation of extra/intracellular fluid and plasma

constituents in the neurosensory retina.[1] Population-based studies estimate that up to 13% of patients with diabetes are affected by DME.[4]

Over the last decade, multiple phase III clinical trials have demonstrated the substantial benefit of intravitreal injection of anti-vascular endothelial growth factor (VEGF) agents in improving visual outcome in eyes with DME.[5–7] Most previous studies have employed either central retinal thickness (CRT) or central subfield thickness (CST) on optical coherence tomography (OCT) as the key anatomic outcome since they are readily accessible and it has generally been accepted that the improvement of these parameters leads to potentially improved visual acuity. However, a wide range of visual acuity can be measured for a given macular thickness as evaluated with CRT or CST,[8–10] reflecting the complex pathophysicology of DME. Although the exact mechanisms of this disconnect between macular thickness and visual acuity have not been fully elucidated, multiple factors seem to play a role including the disturbed foveal photoreceptor integrity,[9–14] center involving disorganization of inner retinal layers (DRIL),[14–16] macular ischemia,[17] the duration of macular thickening, the accumulation of subfoveal hyperreflective foci or hard exudate,[13, 18] or the presence of a premacular posterior hyaloid.[19, 20] Given this background, it is currently considered that macular thickness alone cannot substitute as a reliable surrogate for visual acuity, and its usefulness in assessment of retinal function in clinical practice is limited.

The development of spectral-domain (SD) OCT has allowed better visualization of retinal microstructures in recent years and provided new insights into the management of DME. Numerous studies have demonstrated the potential utility of examining foveal photoreceptor integrity such as an external limiting membrane (ELM) or ellipsoid zone (EZ, also referred to as IS/OS line) as a surrogate biomarker that correlates with visual acuity in eyes with macular diseases, including DME.[9–14, 21–25] However, most studies depended on qualitative assessment or the length of disruption based on several B-scans, and these parameters have not been well validated in the longitudinal follow-up during anti-VEGF therapy. Recent advances in image analysis technology have enabled more advanced assessment of retinal features, including multi-layer retinal segmentation, panmacular EZ integrity mapping, and fluid feature extraction.[26–30] These assessment platforms provide a unique opportunity to evaluate OCT features in eyes with macular disease in a detailed quantitative fashion and assess potential implications as biomarkers for visual function and disease behavior. In addition, given that DME involves a varying degree of extracellular and intracellular fluid accumulation, fluid feature extraction and characterization may enhance the understanding of functional retinal potential and might play an independent role in visual acuity. Herein, this report provides a post-hoc analysis of these higher order OCT retinal parameters in the VISTA-DME study to evaluate the feasibility of quantitative EZ integrity measures as well as intraretinal/subretinal fluid metrics using a unique software platform for retinal layer segmentation and mapping on SD-OCT. In this report, the longitudinal dynamics of EZ integrity, fluid features, and correlation of these metrics with visual acuity are explored.

METHODS

The VISTA-DME study was a multicenter, phase III prospective clinical trial that evaluated the efficacy and the safety of intravitreal aflibercept injection (IAI) compared with laser

photocoagulation in eyes with DME (clinicalTrials.gov identifier).[7, 31, 32] The study was conducted across 54 sites in the United States, according to the principles expressed in the Health Insurance Portability and Accountability Act, the Declaration of Helsinki, and the International Conference on Harmonisation. The local institutional review board approval was secured at each recruitment site before the start of the study. All subjects signed a written informed consent form prior to the enrollment. The principal inclusion criteria were adult patients with type 1 or type 2 diabetes suffering from center involving DME with best corrected visual acuity (BCVA) in ETDRS letter score between 24 and 73 letters (Snellen equivalent, 20/40 to 20/320) in the study eye. Only one eye of each subject was enrolled. Subjects were randomly assigned 1:1:1 to treatment arm with IAI 2.0 mg every 4 weeks (2q4), IAI 8 weeks after 5 initial monthly injections (2q8), or macular laser photocoagulation. From week 24, additional treatment of macular laser photocoagulation was allowed in the IAI arms (2q4 and 2q8) if specific diagnostic criteria were met in the case of disease recurrence or worsening.[31]

Participants

This study was a preliminary post-hoc analysis of the VISTA-DME study including subjects assigned to the IAI arms through week 100 that underwent SD-OCT with the Cirrus HD-OCT (Zeiss, Oberkochen, Germany) platform. Subjects assigned to the macular laser photocoagulation arm were not evaluated in this analysis. For this initial pilot study, exclusion criteria included eyes imaged with the Spectralis OCT (Heidelberg Engineering, Heidelberg, Germany) and eyes that did not have baseline and week 100 macular cube scans of sufficient quality for assessment. The specific time-points analyzed for this study included weeks 0, 4, 8, 12, 16, 20, 24, 28, 52, and 100. The VISTA-DME study included 154 eyes in IAI 2q4 arm and 151 eyes in IAI 2q8 arm (full analysis set).[31] Of these 305 eyes, 138 eyes were evaluated for retinal layer segmentation in this pilot evaluation based on the imaging platform. Two eyes were excluded due to the insufficient image quality of the macular cube at baseline, and 30 eyes were further excluded due to unavailable time-point at week 100.

SD-OCT Image Analysis

Macular cube scans with 512 × 128 A-scans covering a nominal 6 × 6 mm scan area centered on the fixation point, were performed using a Cirrus HD-OCT as part of the VISTA clinical trial. The DICOM-format SD-OCT data was imported into a retinal layer segmentation tool, OCTViewer (Cleveland Clinic, Cleveland, OH) which provided semi-automated segmentation of the internal limiting membrane, ellipsoid zone (EZ), RPE band, intraretinal fluid (IRF) and subretinal fluid (SRF) boundary lines as shown in Figure 1 (bottom row).[23, 26, 33] The segmentation lines created by the software were carefully checked sequentially by 2 masked expert/trained readers, and segmentation errors were manually corrected, as needed. In order to minimize variability, the reading environment was standardized based on location, computer configuration, monitor settings, and lighting configuration. All readers underwent the same training for OCT analysis. In addition, all timepoints of a single subject was reviewed and corrected, as needed, by the same trained reader to minimize inter-timepoint interuserr variation. Following the initial read, the project lead reviewed each scan to confirm consistency and segmentation accuracy. *En face* EZ-RPE macular topographic thickness map was generated to visualize regional EZ alterations and

the severity of loss, as previously described.[21–26] *En face* intraretinal/subretinal fluid map was also generated to visualize regional fluid accumulation. Multiple retinal parameters were subsequently exported and evaluated for analysis, as previously described.[21–26] The central subfield was defined as the inner concentric circle with 0.5 mm radius from the fovea (inner circle on the *en face* map), and the central macular zone was defined as outer concentric circle with 1.0 mm radius from the fovea (outer circle). "Actual" retinal tissue thickness/volume parameters were defined as the "true" retinal tissue thickness/volume through the exclusion of cystic IRF and SRF space with an intention to evaluate the amount of actual retinal tissue, allowing for characterization of retinal thickness independent of cystic fluid. For this analysis, the central macular IRF was analyzed. Retinal fluid index (RFI) was defined as follows; RFI = 100 × IRF volume / (total retinal volume - SRF volume). RFI represents a percentage of IRF volume against retinal volume in a designated area (e.g., central macula), a number ranging between 0% (no IRF) and 100% (total IRF). For instance, the absence of IRF but the presence of SRF was calculated as RFI 0%. Other measurements included the thickness and volume metrics related to the space between photoreceptor EZ band to RPE band (EZ-RPE),[34] the percentage of total EZ attenuation (i.e., the measurement value of EZ-RPE thickness of 0 μm) and partial EZ attenuation (EZ-RPE thickness < 10 μm and < 20 μm) on the *en face* EZ-RPE topographic map.

Statistical Analysis

All statistical analyses were performed using R version 3.4.1 (R Project for Statistical Computing, www.r-project.org). The missing data due to unavailable time-points were excluded from the analysis. The Shapiro-Wilk W-test test was used to evaluate the normality of sample distribution. Continuous variables were analyzed with paired t-test. Correlation analysis was conducted with the Pearson correlation test. In multivariate regression analysis, cubic root transformation of RFI was applied to reduce skewed data distribution, referred to as "transformed RFI." Data are presented as the mean ± standard deviation. All P values were two-tailed, and $P < .05$ was considered statistically significant.

RESULTS

Baseline Characteristics

Overall, 106 eyes of 106 patients were included in this analysis. Specifically, 52 eyes of 52 patients were included in IAI 2q4 arm, and 54 eyes of 54 patients were included in IAI 2q8 arm. Baseline characteristics of patients are presented in Table 1. The mean age at baseline was 62.3 ± 12.0 years (range 26 to 87) in the 2q4 arm and 64.6 ± 8.7 years (range 33 to 81) in the 2q8 arm. The mean BCVA (ETDRS letters) at baseline was 59.0 ± 11.2 letters (Snellen equivalent 20/80) in the 2q4 arm and 58.4 ± 11.6 letters (Snellen 20/70) in the 2q8 arm. The central subfield retinal thickness at baseline was 435 ± 145 μm and 465 ± 143 μm in the 2q4 and 2q8 arm, respectively.

Longitudinal Analysis of EZ Integrity and Fluid Feature Dynamics

Longitudinal changes in BCVA and selected OCT parameters are presented in Figure 2, and longitudinal comparison in BCVA and OCT retinal parameters at week 100 from baseline are shown in Table 2. The BCVA at week 100 significantly improved to 72.6 ± 11.7 letters

(Snellen equivalent 20/32) in the 2q4 arm ($P < .001$) and 71.2 ± 10.9 letters (Snellen equivalent 20/40) in the 2q8 arm ($P < .001$), respectively. Volumetric assessment of OCT retinal parameters was feasible. All EZ-RPE parameters significantly improved from baseline to week 100, including increase in central macular mean EZ-RPE thickness (2q4; 26.6 ± 11.1 μm to 31.6 ± 7.1 μm, $P < .001$, 2q8; 25.2 ± 11.0 μm to 31.4 ± 8.0 μm, $P < .001$), and decrease in the percentage of EZ attenuation (2q4; 11.9 % to 7.0 %, $P < .001$, 2q8; 14.2 % to 8.0 %, $P < .001$).

Fluid parameters reduced during the initial phase of the treatment period and demonstrated significant improvement from baseline to week 100 including decrease in central macular IRF volume (2q4; 0.265 ± 0.257 mm^3 to 0.092 ± 0.210 mm^3, $P < .001$, 2q8; 0.303 ± 0.233 mm^3 to 0.043 ± 0.071 mm^3, $P < .001$) and central macular RFI (2q4; 17.9 % to 7.2 %, $P < .001$, 2q8; 19.8 % to 4.2 %, $P < .001$). Similarly, there was a significant improvement in actual central macular mean retinal tissue thickness, which represents the non-cystic, diffuse thickening of the retinal tissue. At week 100, actual central macular mean retinal tissue thickness was reduced by 20 % and 23 % in the 2q4 arm and 2q8 arm (2q4; 332 ± 48 μm to 266 ± 31 μm, $P < .001$, 2q8; 350 ± 68 μm to 271 ± 31 μm, $P < .001$). Meanwhile, central macular SRF volume was reduced by over 99 % at week 100 in both groups (2q4; 0.011 ± 0.030 mm^3 to $2.3 \times 10^{-5} \pm 1.7 \times 10^{-4}$ mm^3, $P < .001$, 2q8; 0.013 ± 0.039 mm^3 to $7.6 \times 10^{-5} \pm 5.6 \times 10^{-4}$ mm^3, $P < .001$).

Functional and Anatomic Correlation

Correlation between BCVA and OCT retinal parameters at week 100 are shown in Table 3. Multiple EZ-RPE parameters exhibited statistically significant correlation with BCVA, including central subfield EZ-RPE volume (2q4; r = 0.551, $P < .001$, 2q8; r = 0.479, $P < .001$) and central macular mean EZ-RPE thickness (2q4; r = 0.515, $P < .001$, 2q8; 0.437, $P < .001$). A heat map representing the Pearson correlation coefficients between BCVA and OCT retinal parameters from baseline through week 100 is displayed in Figure 3. Beyond week 4, central subfield and central macular EZ-RPE parameters demonstrated a consistent and statistically significant correlation with BCVA. Actual central subfield retinal tissue thickness/volume demonstrated a weak positive correlation in the majority of weeks beyond week 4. Central macular SRF volume did not correlate with BCVA at any time-points. However, there was a weak correlation between changes in central macular SRF volume from baseline to week 100 and visual gain at week 100 (r = −0.214, $P = .028$). In addition, the BCVA at week 100 was significantly higher in eyes with central macular SRF at baseline than eyes without (75.7 ± 11.1 letters vs. 70.4 ± 11.0 letters, $P = .029$). Similarly, although eyes with or without central macular SRF at baseline had comparable BCVA at baseline (58.4 ± 13.2 letters vs. 58.9 ± 10.6 letters, $P = .853$), visual gain at week 100 was significantly higher in eyes with central macular SRF at baseline than eyes without (17.3 ± 12.6 letters vs. 11.5 ± 8.2 letters, $P = .007$). The correlation of baseline SRF and baseline central macular mean EZ-RPE thickness was also significant (r= −0.529, $P < 0.001$). However, it is important to realize the impact of SRF on the visualization of the EZ due to both retinal disruption and the impact on the reflectivity features of the outer retina with the angular changes from the presence of SRF.

Multivariate linear regression analysis on BCVA from baseline to week 100 in all study eyes are presented in Figure 4. Variables included actual central macular mean retinal tissue thickness, central macular mean EZ-RPE thickness, and transformed central macular RFI, selected one from each retinal layer category (e.g., actual retinal tissue thickness, IRF volume, and EZ-RPE thickness) that exhibited statistical significance at most of the observations in Figure 3. Among three variables, central macular mean EZ-RPE thickness exhibited the most robust correlation with BCVA at all time-points from baseline to week 100 (e.g., at week 8, adjusted coefficient 0.743, 95% confidence interval 0.550 to 0.936, $P < .001$). The transformed central macular RFI also independently correlated with BCVA at multiple time-points (e.g., at week 8, adjusted coefficient −4.69, 95% confidence interval −6.79 to −2.58, $P < .001$). Actual central macular mean retinal tissue thickness least correlated with BCVA at given week, the parameter independently correlated with BCVA at week 52 (adjusted coefficient 6.07×10^{-2}, 95% confidence interval 2.53×10^{-3} to 0.119, $P = .041$).

DISCUSSION

In this report, treatment with intravitreal injection of aflibercept resulted in improvement in EZ integrity and quantitative fluid metrics in both 2q4 and 2q8 arms in eyes with DME. Additionally, central subfield and central macular EZ-RPE metrics consistently correlated with BCVA from baseline through week 100 in all study eyes. Multivariate analysis further revealed that two SD-OCT parameters analyzed, central macular mean EZ-RPE thickness and transformed central macular RFI, independently correlated with BCVA at multiple follow-up visits. To the best of our knowledge, this is the first report that quantitatively analyzed retinal fluid metrics on large-scale prospective clinical trial and introduced a potentially novel OCT biomarker “retinal fluid index (RFI).” In addition, this report provides a unique evaluation of “true” retinal tissue in the setting of macular edema. Extracting cystic fluid from the overall measured retinal thickness provides a unique opportunity for insights related to underlying atrophy in the presence of macular edema and may be an important prognostic indicator of visual potential.

As shown in Figure 3 , analysis from this report suggested that the negative correlation between CST and BCVA was modest at baseline when considerable macular thickening was present but became less apparent or non-existent when retinal swelling receded during the course of anti-VEGF therapy, which may help to explain the reason for the wide range of correlation coefficient in previous studies with various degrees of DME.[8–11] Meanwhile, EZ-RPE volumetric parameters consistently exhibited a modest correlation with BCVA throughout the follow-up period. One can estimate the overall positive impact of increasing EZ-RPE thickness on visual acuity, for instance, at week 8, 1 μm increase in central macular mean EZ-RPE thickness had an equivalent of 0.743 ETDRS letters (= adjusted coefficient in multivariate analysis) positive impact in BCVA. Immunohistological evidence suggests that the EZ band represents the mitochondria zone in the photoreceptor inner segment, and the attenuation/loss of EZ band (EZ-RPE thickness) is considered an indicator of the dysfunction of photoreceptors.[34] Our study was in good agreement with previous studies that reported a correlation between visual function and the integrity of the photoreceptor layer in eyes with DME.[9–14] Otani et al retrospectively reviewed SD-OCT cross-sectional

scans in 154 eyes with DME and demonstrated that the length of preserved ELM and photoreceptor inner segment/outer segment junction (currently termed EZ) at the fovea highly correlated with BCVA.[12] Forooghian et al quantitatively assessed the length of photoreceptor outer segment (equivalent to EZ-RPE thickness in our study) on SD-OCT macular cube scans in eyes with DME.[11] Using a prototype algorithm, they reported a statistically significant correlation of mean central subfield photoreceptor outer segment length with visual acuity.[11] Our study has provided concrete evidence that EZ-RPE volumetric parameters correlate with visual acuity regardless of retinal fluid status, and have demonstrated the potential utility of *en face* EZ-RPE mapping that allows unique visualization of EZ attenuation in eyes with DME.

This study demonstrated a novel OCT parameter, termed RFI, to estimate a proportion of IRF volume against total retinal volume. The use of RFI is conceptually attractive as it allows easy estimation of the amount of IRF within the retina. In multivariate analysis, transformed central macular RFI demonstrated a negative correlation with visual acuity in multiple time-points when IRF was relatively abundant supporting the fact that the IRF plays a pivotal role in visual acuity during anti-VEGF therapy. Through an assessment of the predicted impact of RFI on visual acuity, one can estimate the overall negative impact of increasing RFI on visual acuity, Figure 4. As an example, a central macular RFI of 8% at week 8 had an equivalent of 9.4 ETDRS letters $\left(= \sqrt[3]{8} \times -4.69 \right)$ negative impact in BCVA, whereas central macular RFI of 27% had an estimated 14.1 ETDRS letters $\left(= \sqrt[3]{27} \times -4.69 \right)$ negative impact accordingly.

There are several possible explanations for how RFI, which is an indicator of the proportion of IRF volume, might affect visual acuity. First, it is not uncommon to observe a heterogeneous moderate to high reflective signal within the cystic cavities suggestive of protein-rich fluid content which may cause diffraction or the blockage of the light transmission of the neurosensory retina.[35] Second, even if the IRF is observed as a homogeneous low reflective cavity, the misalignment of the Müller cells may interfere with the light transmission within the neurosensory retina.[36] Third, large cystic changes due to high osmotic pressure might induce the stretching of the axons of bipolar cells or photoreceptors beyond their elastic tension limits causing cellular dysfunction and preventing signal transmission from photoreceptors to ganglion cells,[37] perhaps in similar mechanical stress to what has been proposed as the pathophysiology of the DRIL.[16] Finally, a large amount of IRF involving the fovea may also potentially exacerbate tissue hypoxia causing neuronal dysfunction or damage.[17] Recently, Santos et al prospectively studied 21 eyes with DME naïve to anti-VEGF therapy and evaluated the amount of IRF using lower optical reflectivity ratio as a surrogate on a Cirrus HD-OCT platform.[38] The authors found increased optical reflectivity within the inner nuclear layer, outer plexiform layer, and outer segment one week after intravitreal ranibizumab injection significantly correlated with the improvement in visual acuity at one month, which may support the findings in the present study that RFI affected visual acuity.[38]

The quantitative analysis on IRF/SRF volume also allowed us to evaluate the actual retinal tissue thickness/volume parameters that may account for non-cystic, diffuse thickening of

the retinal tissue. IRF volume reflects the amount of fluid accumulated in extracellular space mostly in the inner nuclear layer and the outer plexiform layer while diffuse thickening of retinal tissue reflects the amount of intracellular fluid due to swelling of the glial cells.[39, 40] In some ways counter to expectations, actual mean retinal tissue thickness parameters exhibited a weak but positive correlation with BCVA beyond week 4, suggesting that eyes with thinner retina had worse BCVA. This suggests that extracting the cystic fluid volume from the overall retinal volume enables identification of latent atrophic changes in some eyes that has negative visual consequence. It may be argued that overestimation (i.e., false positive) of IRF volume that could have occurred due to shadowing effect during the segmentation process led to the underestimation of actual mean retinal tissue thickness, however, this was unlikely beyond week 20 considering the dramatic decrease in IRF after the initial monthly treatments. Underlying atrophy may have been more present in this study than in treatment naïve patients since approximately 40% of eyes in the VISTA-DME study had been treated with anti-VEGF therapy prior to enrollment.[31] Also, some eyes with over 400 microns in actual retinal tissue thickness with good BCVA (e.g., over 80 ETDRS letters, Figure 5) suggested that in addition to the importance of underlying healthy retinal tissue, non-cystic, sponge-like retinal thickening might not be as influential for visual acuity in eyes with DME. Previously, Pelosini et al evaluated 129 eyes with cystoid macular edema and measured the area of retinal tissue bridging inner and outer plexiform layers on SD-OCT C-scans, which potentially represents bipolar axons and Müller cells responsible for visual transmission pathway.[41] That study demonstrated measuring the bridging retinal tissue within central 2 mm of the macula explained 80.7% of the variation in BCVA.[41] This model was based on a cross-sectional study and its applicability during anti-VEGF therapy is unknown. These results support the need for additional research into the key components of retinal integrity related to visual acuity function, including approaches to image analysis.

Central macular SRF volume dramatically reduced with IAI treatment. Although central macular SRF volume did not correlate with BCVA at any given time-points, the final BCVA and the visual gain at week 100 compared to baseline were significantly higher in eyes with central macular SRF at baseline than eyes without when baseline BCVA were comparable. These results were in line with the post-hoc analyses of other randomized clinical trials suggesting that the presence of SRF was prognostic of better visual outcomes in eyes with DME treated with anti-VEGF therapy.[42, 43]

The results from our univariate and multivariate analysis might suggest that high central macular RFI is more detrimental to BCVA than central macular diffuse retinal thickening. It has been postulated that there may be a threshold effect in retinal thickening that causes neural damage,[44] as was also observed in the VISTA-DME study where a small rebound of central retinal thickness in the 2q8 arm beyond week 24 did not seem to affect the final visual outcome.[7, 32] Based on an assumption that small cystic changes distort neurons without surpassing their mechanical limits,[44] it is hypothesized that there may be a threshold effect in central macular RFI that accelerates mechanical cellular damage or induces snapping of the bipolar cell or photoreceptor axons, and in this context, RFI might potentially serve as a “stretching index” of the macular tissues. Further research is needed to elucidate the relationship between OCT microstructural parameters and visual acuity in eyes with DME.

This study has important strengths and limitations that should be acknowledged. Selected strengths of the current study include the prospective randomized design of VISTA-DME study, long-term follow-up with numerous time-points, masked examiners, and a uniform treatment regimen. This study has several limitations that should be mentioned. This subanalysis was a post-hoc exploratory approach with a smaller pilot sample size than the original study. Due to the specifications of the OCT retinal layer segmentation tool, it is possible that retinal thickness/volume may be slightly overestimated since retinal thickness was measured parallel to the vertical axis of the OCT image and not uniformly perpendicular to retinal surface or RPE.[33, 45] During the retinal layer segmentation process, the shadowing effect caused by marked retinal swelling at times made it challenging to determine the exact boundary lines for intraretinal cystic fluid and EZ band which may have led to inaccurate evaluation of IRF and EZRPE metrics. However, when considering the correlation with visual acuity, shadowing effect may not be problematic for assessing EZ because if SD-OCT infrared light source is unable to depict EZ band, visible light reaching photoreceptor may be proportionally attenuated affecting visual acuity. In addition, the IRF volume may have been slightly overestimated as speckle noise degraded the image quality of unaveraged single cross-sectional OCT occasionally confounding small IRF.[46] The modification of SD-OCT image acquisition software that allows averaging of multiple scans for the entire macular cube may reduce speckle noise and improve the accuracy of retinal layer segmentation.

An additional limitation of this study is that the current methods used represent research-based software that is not practical for widespread clinical use at this time. Ongoing refinement of the software, including the introduction of deep learning, will hopefully enable more widespread utilization of this technology in vitreoretinal clinics.[47] Future opportunities for additional analysis will include the incorporation of additional biomarkers/variables such as DRIL, hyperreflective foci, signal intensity within the IRF, and the duration of DME with the entire VISTA-DME dataset, including eyes imaged with the Spectralis OCT which may allow us to explore and identify potential imaging biomarkers that predict visual outcome. In addition, examining the laser arm of the phase III study may also enable addition insights into retinal dynamics in response to anti-VEGF therapy.

In conclusion, this study demonstrates the feasibility of volumetric assessment of fluid features in DME and quantitative assessment of EZ integrity. Multiple features provided correlation with visual acuity during anti-VEGF therapy. IRF and SRF volume decreased during the period of the initial 5 monthly injections in the majority of eyes. In multivariate analysis, central macular mean EZ-RPE thickness and central macular RFI independently correlated with BCVA at multiple follow-up visits, indicating as a potential quantitative biomarkers for monitoring visual function in eyes with DME. Future research will be focused on identifying potential imaging biomarkers that may help predict required treatment frequency.

Grant Support:

Regeneron (JPE); NIH/NEI K23-EY022947–01A1 (JPE); Research to Prevent Blindness (Cole Eye Institutional Grant); Unrestricted travel grant from Alcon Novartis Hida Memorial Award 2015 funded by Alcon Japan Ltd (AU); Betty J. Powers Retina Research Fellowship (AU)

Statement Related to Financial Support: The authors had full control of study design, all data, and manuscript drafting.

REFERENCES

1. Antonetti DA, Klein R, Gardner TW. Diabetic retinopathy. N Engl J Med 2012;366:1227–39. [PubMed: 22455417]
2. NCD Risk Factor Collaboration (NCD-RisC). Worldwide trends in diabetes since 1980: a pooled analysis of 751 population-based studies with 4.4 million participants. Lancet 2016;387:1513–30. [PubMed: 27061677]
3. Yau JW, Rogers SL, Kawasaki R, et al. Global prevalence and major risk factors of diabetic retinopathy. Diabetes Care 2012;35:556–64. [PubMed: 22301125]
4. Lee R, Wong TY, Sabanayagam C. Epidemiology of diabetic retinopathy, diabetic macular edema and related vision loss. Eye Vis (Lond) 2015;2:17. [PubMed: 26605370]
5. Elman MJ, Aiello LP, Beck RW, et al. Randomized trial evaluating ranibizumab plus prompt or deferred laser or triamcinolone plus prompt laser for diabetic macular edema. Ophthalmology 2010;117:1064–1077 e35. [PubMed: 20427088]
6. Brown DM, Nguyen QD, Marcus DM, et al. Long-term outcomes of ranibizumab therapy for diabetic macular edema: the 36-month results from two phase III trials: RISE and RIDE. Ophthalmology 2013;120:2013–22. [PubMed: 23706949]
7. Heier JS, Korobelnik JF, Brown DM, et al. Intravitreal Aflibercept for Diabetic Macular Edema: 148-Week Results from the VISTA and VIVID Studies. Ophthalmology 2016;123:2376–2385. [PubMed: 27651226]
8. Browning DJ, Glassman AR, Aiello LP, et al. Relationship between optical coherence tomography-measured central retinal thickness and visual acuity in diabetic macular edema. Ophthalmology 2007;114:525–36. [PubMed: 17123615]
9. Maheshwary AS, Oster SF, Yuson RM, Cheng L, Mojana F, Freeman WR. The association between percent disruption of the photoreceptor inner segment-outer segment junction and visual acuity in diabetic macular edema. Am J Ophthalmol 2010;150:63–67 e1. [PubMed: 20451897]
10. Alasil T, Keane PA, Updike JF, et al. Relationship between optical coherence tomography retinal parameters and visual acuity in diabetic macular edema. Ophthalmology 2010;117:2379–86. [PubMed: 20561684]
11. Forooghian F, Stetson PF, Meyer SA, et al. Relationship between photoreceptor outer segment length and visual acuity in diabetic macular edema. Retina 2010;30:63–70. [PubMed: 19952996]
12. Otani T, Yamaguchi Y, Kishi S. Correlation between visual acuity and foveal microstructural changes in diabetic macular edema. Retina 2010;30:774–80. [PubMed: 19996821]
13. Uji A, Murakami T, Nishijima K, et al. Association between hyperreflective foci in the outer retina, status of photoreceptor layer, and visual acuity in diabetic macular edema. Am J Ophthalmol 2012;153:710–7, 717 e1. [PubMed: 22137207]
14. Das R, Spence G, Hogg RE, Stevenson M, Chakravarthy U. Disorganization of Inner Retina and Outer Retinal Morphology in Diabetic Macular Edema. JAMA Ophthalmol 2018;136:202–208. [PubMed: 29327033]
15. Radwan SH, Soliman AZ, Tokarev J, Zhang L, van Kuijk FJ, Koozekanani DD. Association of Disorganization of Retinal Inner Layers With Vision After Resolution of Center-Involved Diabetic Macular Edema. JAMA Ophthalmol 2015;133:820–5. [PubMed: 25950417]
16. Sun JK, Lin MM, Lammer J, et al. Disorganization of the retinal inner layers as a predictor of visual acuity in eyes with center-involved diabetic macular edema. JAMA Ophthalmol 2014;132:1309–16. [PubMed: 25058813]
17. Murakami T, Nishijima K, Sakamoto A, Ota M, Horii T, Yoshimura N. Foveal cystoid spaces are associated with enlarged foveal avascular zone and microaneurysms in diabetic macular edema. Ophthalmology 2011;118:359–67. [PubMed: 20656355]
18. Otani T, Kishi S. Tomographic findings of foveal hard exudates in diabetic macular edema. Am J Ophthalmol 2001;131:50–4. [PubMed: 11162979]

19. Kaiser PK, Riemann CD, Sears JE, Lewis H. Macular traction detachment and diabetic macular edema associated with posterior hyaloidal traction. Am J Ophthalmol 2001;131:44–9. [PubMed: 11162978]
20. Lewis H, Abrams GW, Blumenkranz MS, Campo RV. Vitrectomy for diabetic macular traction and edema associated with posterior hyaloidal traction. Ophthalmology 1992;99:753–9. [PubMed: 1594222]
21. Ugwuegbu O, Uchida A, Singh RP, et al. Quantitative assessment of outer retinal layers and ellipsoid zone mapping in hydroxychloroquine retinopathy. Br J Ophthalmol 2019;103:3–7. [PubMed: 30190364]
22. Banaee T, Singh RP, Champ K, et al. Ellipsoid Zone Mapping Parameters In Retinal Venous Occlusive Disease With Associated Macular Edema. Ophthalmology Retina 2018;2:836–841. [PubMed: 30221215]
23. Arepalli S, Traboulsi EI, Ehlers JP. Ellipsoid Zone Mapping and Outer Retinal Assessment in Stargardt Disease. Retina 2018;38:1427–1431. [PubMed: 28613213]
24. Runkle AP, Kaiser PK, Srivastava SK, Schachat AP, Reese JL, Ehlers JP. OCT Angiography and Ellipsoid Zone Mapping of Macular Telangiectasia Type 2 From the AVATAR Study. Invest Ophthalmol Vis Sci 2017;58:3683–3689. [PubMed: 28727884]
25. Itoh Y, Ehlers JP. Ellipsoid Zone Mapping and Outer Retinal Characterization after Intravitreal Ocriplasmin. Retina 2016;36:2290–2296. [PubMed: 27341665]
26. Itoh Y, Vasanji A, Ehlers JP. Volumetric ellipsoid zone mapping for enhanced visualisation of outer retinal integrity with optical coherence tomography. Br J Ophthalmol 2016;100:295–9. [PubMed: 26201354]
27. Xu D, Yuan A, Kaiser PK, et al. A novel segmentation algorithm for volumetric analysis of macular hole boundaries identified with optical coherence tomography. Invest Ophthalmol Vis Sci 2013;54:163–9. [PubMed: 23221077]
28. Kashani AH, Keane PA, Dustin L, Walsh AC, Sadda SR. Quantitative subanalysis of cystoid spaces and outer nuclear layer using optical coherence tomography in age-related macular degeneration. Invest Ophthalmol Vis Sci 2009;50:3366–73 [PubMed: 19168893]
29. Breger A, Ehler M, Bogunovic H, et al. Supervised learning and dimension reduction techniques for quantification of retinal fluid in optical coherence tomography images. Eye (Lond) 2017;31:1212–1220. [PubMed: 28430181]
30. Chakravarthy U, Goldenberg D, Young G, et al. Automated Identification of Lesion Activity in Neovascular Age-Related Macular Degeneration. Ophthalmology 2016;123:1731–1736. [PubMed: 27206840]
31. Korobelnik JF, Do DV, Schmidt-Erfurth U, et al. Intravitreal aflibercept for diabetic macular edema. Ophthalmology 2014;121:2247–54. [PubMed: 25012934]
32. Brown DM, Schmidt-Erfurth U, Do DV, et al. Intravitreal Aflibercept for Diabetic Macular Edema: 100-Week Results From the VISTA and VIVID Studies. Ophthalmology 2015;122:2044–52. [PubMed: 26198808]
33. Uchida A, Pillai JA, Bermel R, et al. Outer Retinal Assessment using Spectral Domain Optical Coherence Tomography in Patients with Alzheimer's and Parkinson's Disease. Invest Ophthalmol Vis Sci 2018;59:2768–2777. [PubMed: 29860463]
34. Cuenca N, Ortuno-Lizaran I, Pinilla I. Cellular Characterization of Optical Coherence Tomography and Outer Retinal Bands Using Specific Immunohistochemistry Markers and Clinical Implications. Ophthalmology 2017.
35. Murakami T, Yoshimura N. Structural changes in individual retinal layers in diabetic macular edema. J Diabetes Res 2013;2013:920713. [PubMed: 24073417]
36. Franze K, Grosche J, Skatchkov SN, et al. Muller cells are living optical fibers in the vertebrate retina. Proc Natl Acad Sci U S A 2007;104:8287–92. [PubMed: 17485670]
37. Marmor MF. Mechanisms of fluid accumulation in retinal edema. Doc Ophthalmol 1999;97:239–49. [PubMed: 10896337]
38. Santos AR, Alves D, Santos T, Figueira J, Silva R, Cunha-Vaz JG. Measurements of retinal fluid by OCT leakage in diabetic macular edema: A biomarker of visual acuity response to treatment. Retina 2019;39:52–60. [PubMed: 29077605]

39. Bolz M, Ritter M, Schneider M, Simader C, Scholda C, Schmidt-Erfurth U. A systematic correlation of angiography and high-resolution optical coherence tomography in diabetic macular edema. Ophthalmology 2009;116:66–72. [PubMed: 19118697]
40. Yanoff M, Fine BS, Brucker AJ, Eagle RC Jr. Pathology of human cystoid macular edema. Surv Ophthalmol 1984;28 Suppl:505–11. [PubMed: 6463850]
41. Pelosini L, Hull CC, Boyce JF, McHugh D, Stanford MR, Marshall J. Optical coherence tomography may be used to predict visual acuity in patients with macular edema. Invest Ophthalmol Vis Sci 2011;52:2741–8. [PubMed: 20538987]
42. Sophie R, Lu N, Campochiaro PA. Predictors of Functional and Anatomic Outcomes in Patients with Diabetic Macular Edema Treated with Ranibizumab. Ophthalmology 2015;122:1395–401. [PubMed: 25870079]
43. Bressler SB, Qin H, Beck RW, et al. Factors associated with changes in visual acuity and central subfield thickness at 1 year after treatment for diabetic macular edema with ranibizumab. Arch Ophthalmol 2012;130:1153–61. [PubMed: 22965591]
44. Grewal DS, Hariprasad SM, Jaffe GJ. Role of Disorganization of Retinal Inner Layers as an Optical Coherence Tomography Biomarker in Diabetic and Uveitic Macular Edema. Ophthalmic Surg Lasers Imaging Retina 2017;48:282–288. [PubMed: 28419393]
45. Hariri A, Lee SY, Ruiz-Garcia H, Nittala MG, Heussen FM, Sadda SR. Effect of angle of incidence on macular thickness and volume measurements obtained by spectral-domain optical coherence tomography. Invest Ophthalmol Vis Sci 2012;53:5287–91. [PubMed: 22859741]
46. Schmitt JM, Xiang SH, Yung KM. Speckle in optical coherence tomography. J Biomed Opt 1999;4:95–105. [PubMed: 23015175]
47. Schlegl T, Waldstein SM, Bogunovic H, et al. Fully Automated Detection and Quantification of Macular Fluid in OCT Using Deep Learning. Ophthalmology 2018;125:549–558. [PubMed: 29224926]

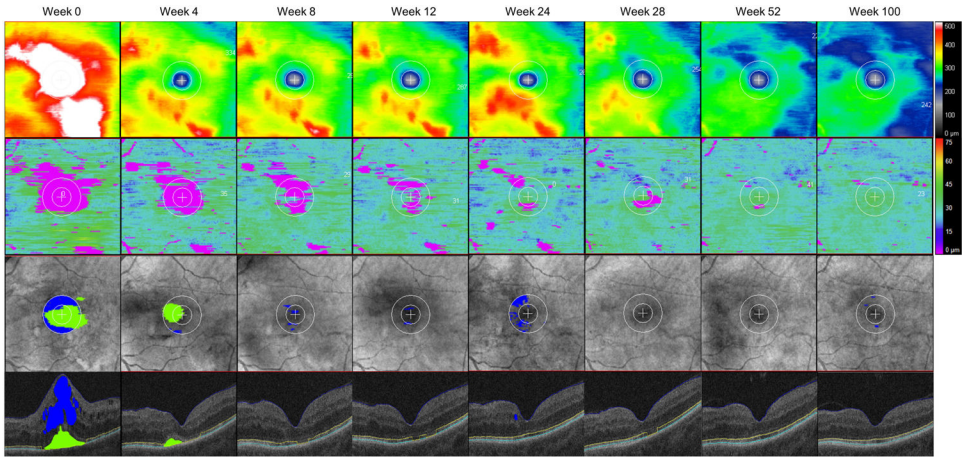

Figure 1. A representative case with diabetic macular edema treated with intravitreal aflibercept injection demonstrating a longitudinal change in *en face* retinal thickness mapping, ellipsoid zone (EZ) mapping, intraretinal/subretinal fluid mapping, and horizontal OCT B-scan image.

The left eye from a 51-year-old female patient in the 2q4 arm. Among 10 follow-up time points that have been evaluated in this subanalysis, 8 selected time points are shown in the figure including the baseline (farthest left column), week 4, 8, 12, 24 28, 52 and 100 (farthest right column). An inner circle represents the macular radius of 0.5 mm (corresponds to central subfield) and an outer circle represents the macular radius of 1.0 mm (corresponds to central macula) in *en face* macular map. (**Top row**) *En face* retinal thickness mapping. (**Second row**) *En face* EZ mapping representing the topographical thickness between EZ and retinal pigment epithelium (RPE). EZ-RPE attenuation mainly localized within the central macular area gradually decreased its size through week 52. (**Third row**) Intraretinal and subretinal fluid mapping. Intraretinal fluid within central macula (an area filled in blue) and subretinal fluid (an area filled in green). (**Bottom row**) Horizontal B-scan crossing the central fovea displaying semi-automatically segmented retinal layer boundaries and visually discernable fluid. The internal limiting membrane (blue line), EZ band (yellow line), RPE (turquoise line), intraretinal fluid within central macula (an area filled in blue) and subretinal fluid (an area filled in green). Each boundary was verified by trained reviewers, and segmentation errors were carefully corrected manually.

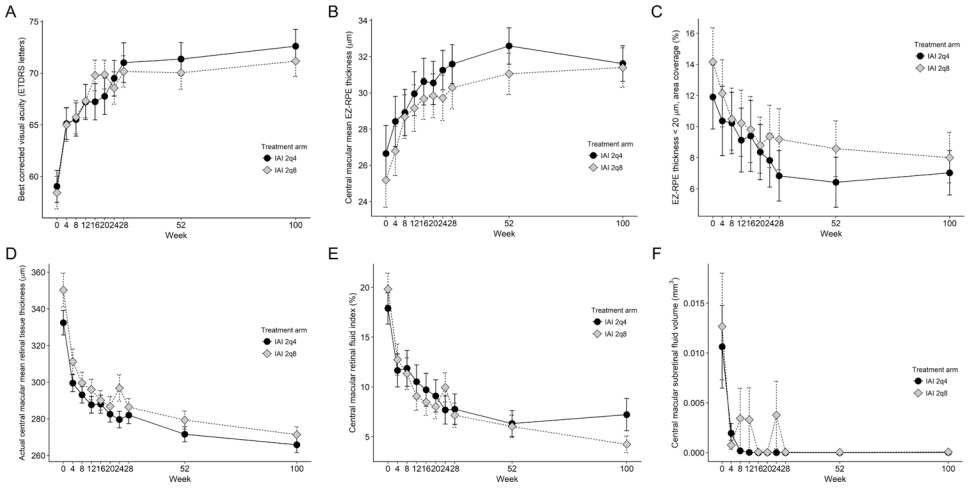

Figure 2. Longitudinal changes in best corrected visual acuity and selected OCT parameters from baseline to week 100 in 2q4 and 2q8 arms.

2q4 arm received intravitreal aflibercept injection (IAI) every 4 weeks from baseline to week 100, while 2q8 am received IAI every 4 weeks from baseline to week 16 (5 injections) followed by dosing every 8 weeks through week 100. The error bars indicate the standard errors of the mean. **A**, Mean change in best corrected visual acuity (ETDRS letters) from baseline through week 100 in 2q4 and 2q8 arms. **B**, Central macular mean ellipsoid zone (EZ) to retinal pigment epithelium (RPE) thickness. **C,** The area coverage of EZ-RPE thickness < 20 μm. **D,** Actual central macular mean retinal tissue thickness. **E,** Central macular retinal fluid index. **F,** Central macular subretinal fluid volume.

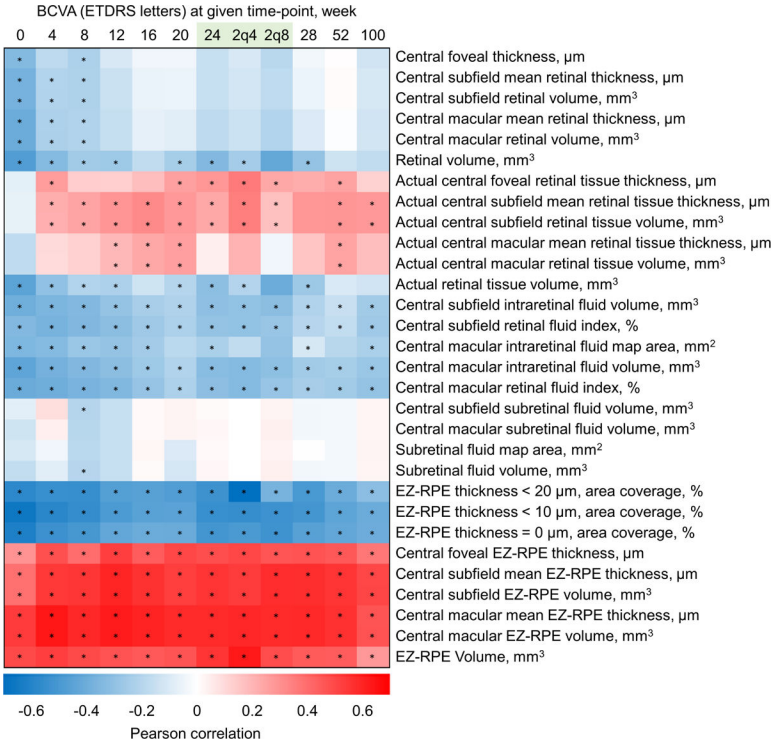

Figure 3. A heat map representing the Pearson correlation coefficients between best corrected visual acuity (ETDRS letters) and OCT retinal parameters from baseline through week 100.

Each colored rectangle represents the degree of correlation coefficient at specific week; positive correlations are filled in red whereas negative correlations are filled in blue. Correlation coefficients are depicted according to the shown color scale shown at the bottom. Superimposed asterisk indicates the statistical significance of $P < .05$. At week 24, separate 2q4 and 2q8 arms are also shown. Central subfield and central macular ellipsoid zone (EZ) to retinal pigment epithelium (RPE) parameters demonstrate a consistent moderate correlation with best corrected visual acuity (BCVA) at given week. Actual central subfield and central macular retinal tissue thickness/volume parameters demonstrate a weak positive correlation beyond week 4.

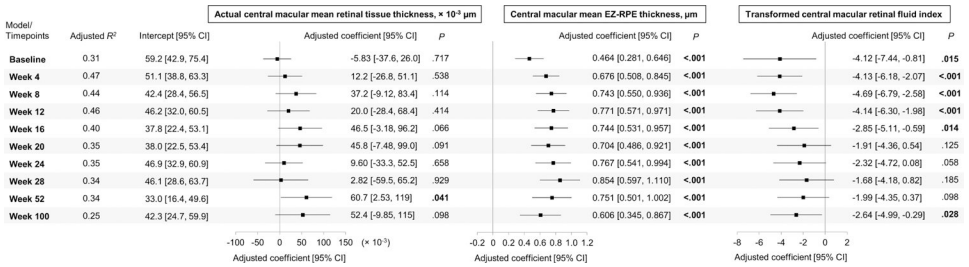

Figure 4. Multivariate linear regression analysis on BCVA (ETDRS letters) from baseline to week 100 in all study eyes.

Independent variables included actual central macular mean retinal tissue thickness, central macular mean ellipsoid zone (EZ) to retinal pigment epithelium (RPE) thickness, and transformed central macular retinal fluid index. Adjusted R-squared (R^2), a forest plot, adjusted coefficient with 95% confidence interval (CI) and *P* values for each variable at given week are shown. *P* values in bold letters indicate statistical significance of less than .05.

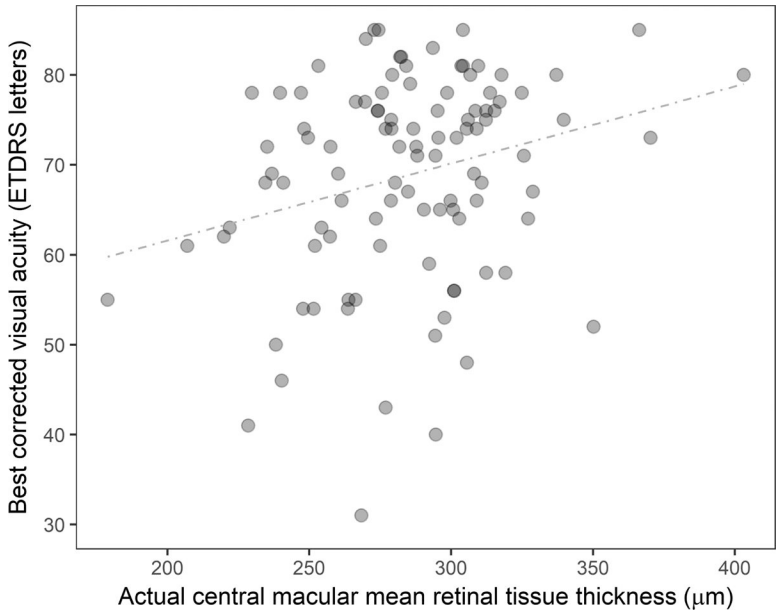

Figure 5. Scatterplot showing the relationship between actual central macular mean retinal tissue thickness and best corrected visual acuity (ETDRS letters) at week 20 (include both 2q4 and 2q8 arms).

The actual mean retinal tissue thickness represents mean retinal tissue thickness excluding both intraretinal and subretinal fluid (i.e., equivalent to the mean retinal thickness of diffuse, non-cystic retinal thickening). The graph demonstrate a weak positive correlation between two parameters (the regression coefficient is r = 0.264, $P = .007$) at week 20.

Table 1.

Baseline characteristics of patients

	IAI 2q4	IAI 2q8	All IAI
Number of eyes, *n*	52	54	106
Age, years	62.3 ± 12.0	64.6 ± 8.7	63.5 ± 10.5
Gender, female, *n* (%)	25 (48%)	31 (57%)	56 (53%)
HbAlc, %	7.8 ± 1.9	7.7 ± 1.5	7.7 ± 1.7
Diastolic blood pressure, mmHg	73.9 ± 8.0	75.0 ± 8.7	74.4 ± 8.4
Systolic blood pressure, mmHg	132.4 ± 17.5	134.8 ± 15.3	133.6 ± 16.5
BCVA, ETDRS letters	59.0 ± 11.2	58.4 ± 11.6	58.7 ± 11.3
Central subfield retinal thickness, μm	435 ± 145	465 ± 143	450 ± 144

Abbreviations: BCVA, best corrected visual acuity; ETDRS, early treatment diabetic retinopathy study; IAI, intravitreal aflibercept injection.

Central subfield is equivalent to a distance of 0.5 mm from the fovea (inner circle on *en face* mapping).

Table 2.

Longitudinal comparison of visual acuity and OCT retinal parameters between baseline and week 100.

	IAI 2q4 *n* = 52		*P*	IAI 2q8 *n* = 54		*P*
	Baseline	**Week 100**		**Baseline**	**Week 100**	
BCVA, ETDRS letters	59.0 ± 11.2	72.6 ± 11.7	< **.001**	58.4 ± 11.6	71.2 ± 10.9	< **.001**
Central foveal thickness, μm	437±181	227 ± 128	< **.001**	460 ±177	199 ± 85	< **.001**
Central subfield mean retinal thickness, μm	435±145	267±101	< **.001**	465 ±143	249 ± 60	< **.001**
Central subfield retinal volume, mm^3	0.34 ± 0.11	0.21 ± 0.08	< **.001**	0.36 ± 0.11	0.19 ± 0.05	< **.001**
Central macular mean retinal thickness, μm	420± 113	295 ± 79	< **.001**	451± 112	285 ± 43	< **.001**
Central macular retinal volume, mm^3	1.32 ± 0.35	0.93 ± 0.25	< **.001**	1.42 ± 0.35	0.90 ± 0.13	< **.001**
Retinal volume, mm^3	11.8 ± 2.3	9.8 ± 1.2	< **.001**	12.4 ± 2.2	9.8 ± 0.9	< **.001**
Actual central foveal retinal tissue thickness, μm	220 ± 79	170 ± 48	< **.001**	247 ± 113	178 ± 62	< **.001**
Actual central subfield mean retinal tissue thickness, μm	289 ± 53	221 ± 35	< **.001**	300 ± 73	225 ± 37	< **.001**
Actual central subfield retinal tissue volume, mm^3	0.23 ± 0.04	0.17 ± 0.03	< **.001**	0.23 ± 0.06	0.18 ± 0.03	< **.001**
Actual central macular mean retinal tissue thickness,	332 ± 48	266 ± 31	< **.001**	350 ± 68	271 ± 31	< **.001**
Actual central macular retinal tissue volume, mm^3	1.05 ± 0.15	0.84 ± 0.10	< **.001**	1.10 ± 0.21	0.85 ± 0.10	< **.001**
Actual retinal tissue volume, mm^3	11.5 ± 2.0	9.6 ± 1.0	< **.001**	12.0 ± 2.1	9.7 ± 0.9	< **.001**
Central subfield intraretinal fluid volume, mm^3	0.108 ± 0.105	0.037 ± 0.075	< **.001**	0.122 ± 0.088	0.019 ± 0.035	< **.001**
Central subfield retinal fluid index, %	27.7 ± 17.5	12.0 ± 17.4	< **.001**	31.0 ± 16.0	7.7 ± 11.2	< **.001**
Central macular intraretinal fluid map area, mm^2	2.02 ± 0.72	1.06 ± 0.88	< **.001**	2.13 ± 0.69	0.75 ± 0.73	< **.001**
Central macular intraretinal fluid volume, mm^3	0.265 ± 0.257	0.092 ± 0.210	< **.001**	0.303 ± 0.233	0.043 ± 0.071	< **.001**
Central macular retinal fluid index, %	17.9 ± 11.4	7.2 ± 11.7	< **.001**	19.8 ± 11.8	4.2 ± 6.1	< **.001**
Central subfield subretinal fluid volume, mm^3	0.007 ± 0.018	$2.3 \times 10^{-5} \pm 1.7 \times 10^{-4}$	**.010**	0.007 ± 0.019	$7.6 \times 10^{-5} \pm 5.6 \times 10^{-4}$	**.008**
Central macular subretinal fluid volume, mm^3	0.011 ± 0.030	$2.3 \times 10^{-5} \pm 1.7 \times 10^{-4}$	**.014**	0.013 ± 0.039	$7.6 \times 10^{-5} \pm 5.6 \times 10^{-4}$	**.022**
Subretinal fluid map area, mm^2	0.198 ± 0.514	0.001 ± 0.010	**.008**	0.261 ± 0.662	0.004 ± 0.028	**.006**
Subretinal fluid volume, mm^3	0.011 ± 0.031	$2.3 \times 10^{-5} \pm 1.7 \times 10^{-4}$	**.014**	0.016 ± 0.052	$7.6 \times 10^{-5} \pm 5.6 \times 10^{-4}$	**.032**
Central foveal EZ-RPE thickness, μm	25.8 ± 19.3	35.5 ± 13.9	**.007**	23.1 ± 22.8	34.0 ± 16.5	**.001**
Central subfield mean EZ-RPE thickness, μm	25.3 ± 14.1	33.0 ± 8.4	< **.001**	22.9 ± 14.2	32.5 ± 9.8	< **.001**
Central subfield EZ-RPE volume, mm^3	0.020 ± 0.011	0.026 ± 0.007	< **.001**	0.018 ± 0.011	0.025 ± 0.008	< **.001**
Central macular mean EZ-RPE thickness, μm	26.6 ± 11.1	31.6 ± 7.1	< **.001**	25.2 ± 11.0	31.4 ± 8.0	< **.001**
Central macular EZ-RPE volume, mm^3	0.084 ± 0.035	0.099 ± 0.022	< **.001**	0.079 ± 0.035	0.099 ± 0.025	< **.001**

	IAI 2q4 *n* = 52		*P*	IAI 2q8 *n* = 54		*P*
	Baseline	**Week 100**		**Baseline**	**Week 100**	
EZ-RPE Volume, mm^3	1.05 ± 0.18	1.09 ± 0.15	**.013**	1.04 ± 0.20	1.10 ± 0.18	**< .001**
EZ-RPE thickness < 20 μm, area coverage (%)	11.9 ± 14.9	7.0 ± 10.3	**< .001**	14.2 ± 16.1	8.0 ± 12.0	**< .001**
EZ-RPE thickness < 10 μm, area coverage (%)	7.7 ± 10.4	4.2 ± 8.0	**.002**	8.7 ± 9.4	4.7 ± 6.8	**< .001**
EZ-RPE thickness = 0 μm, area coverage (%)	7.0 ± 9.8	3.9 ± 7.8	**.002**	8.1 ± 9.1	4.5 ± 6.6	**< .001**

Abbreviations: BCVA, best corrected visual acuity; ETDRS, Early Treatment Diabetic Retinopathy Study; EZ, ellipsoid zone; IAI, intravitreal aflibercept injection; RPE, retinal pigment epithelium.

Central subfield is equivalent to 0.5 mm distant from the fovea (inner circle on *en face* mapping).

Central macula is equivalent to 1.0 mm distant from the fovea (outer circle on *en face* mapping).

Statistical analysis conducted with the paired t-test.

P values in bold text are statistically significant at $P < .05$.

Table 3.

Correlation between BCVA (ETDRS letters) and OCT retinal parameters at week 100.

	IAI 2q4		IAI 2q8	
	Coefficient	***P***	**Coefficient**	***P***
Central foveal thickness, μm	−0.09	.526	−0.219	.112
Central subfield mean retinal thickness, μm	−0.132	.353	−0.102	.465
Central subfield retinal volume, mm^3	−0.128	.364	−0.102	.465
Central macular mean retinal thickness, μm	−0.142	.314	−0.131	.346
Central macular retinal volume, mm^3	−0.138	.33	−0.131	.346
Retinal volume, mm^3	−0.070	.621	−0.302	**.026**
Actual central foveal retinal tissue thickness, μm	0.397	**.004**	−0.081	.562
Actual central subfield mean retinal tissue thickness, μm	0.339	**.014**	0.24	.081
Actual central subfield retinal tissue volume, mm^3	0.34	**.014**	0.24	.081
Actual central macular mean retinal tissue thickness, μm	0.251	.073	0.12	.388
Actual central macular retinal tissue volume, mm^3	0.261	.062	0.12	.388
Actual retinal tissue volume, mm^3	0.009	.952	−0.28	**.041**
Central subfield intraretinal fluid volume, mm^3	−0.259	.064	−0.334	**.014**
Central subfield retinal fluid index, %	−0.232	.098	−0.353	**.009**
Central macular intraretinal fluid map area, mm^2	−0.187	.184	−0.32	**.019**
Central macular intraretinal fluid volume, mm^3	−0.284	**.041**	−0.41	**.002**
Central macular retinal fluid index, %	−0.269	.054	−0.408	**.002**
Central subfield subretinal fluid volume, mm^3	0.090	.528	0.023	.867
Central macular subretinal fluid volume, mm^3	0.090	.528	0.023	.867
Subretinal fluid map area, mm^2	0.090	.528	0.023	.867
Subretinal fluid volume, mm^3	0.090	.528	0.023	.867
Central foveal EZ-RPE thickness, μm	0.321	**.020**	0.422	**.001**
Central subfield mean EZ-RPE thickness, μm	0.543	< **.001**	0.479	< **.001**
Central subfield EZ-RPE volume, mm^3	0.551	< **.001**	0.479	< **.001**
Central macular mean EZ-RPE thickness, μm	0.515	< **.001**	0.437	< **.001**
Central macular EZ-RPE volume, mm^3	0.519	< **.001**	0.437	< **.001**
EZ-RPE Volume, mm^3	0.381	**.005**	0.207	.134
EZ-RPE thickness < 20 μm, area coverage, %	−0.489	< **.001**	−0.163	.238
EZ-RPE thickness < 10 μm, area coverage, %	−0.458	< **.001**	−0.339	**.012**
EZ-RPE thickness = 0 μm, area coverage, %	−0.442	**.001**	−0.342	.011

Abbreviations: BCVA, best-corrected visual acuity; ETDRS, Early Treatment Diabetic Retinopathy Study; EZ, ellipsoid zone; IAI, intravitreal aflibercept injection; RPE, retinal pigment epithelium.

Central subfield is equivalent to 0.5 mm distant from the fovea (inner circle on *en face* mapping).

Central macula is equivalent to 1.0 mm distant from the fovea (outer circle on *en face* mapping).

Statistical analysis conducted with the Pearson correlation.

P values in bold text are statistically significant at $P < .05$.